A CLASS OF ASYMPTOTICALLY OPTIMUM ITERATED-DECISION MULTIUSER DETECTORS

Albert M. Chan and Gregory W. Wornell

Research Laboratory of Electronics
MIT, Cambridge, MA 02139
{chanal,gww}@allegro.mit.edu

ABSTRACT

A promising class of nonlinear multiuser detectors is introduced for CDMA systems. These "iterated-decision" multiuser detectors use optimized multipass algorithms to successively cancel multiple-access interference (MAI) from received data and generate symbol decisions whose reliability increases monotonically with each iteration. They significantly outperform decorrelating detectors and linear minimum mean-square error (MMSE) multiuser detectors, but have the same order of computational complexity. When the ratio of the number of users to the spreading factor is below a certain threshold, iterated-decision multiuser detectors asymptotically achieve the performance of the "optimum" multiuser detector, i.e., maximum-likelihood (ML) decoding.

1. INTRODUCTION

A variety of multiuser detectors have been proposed for CDMA channels over the last decade and a half as solutions to the problem of mitigating multiple-access interference (MAI) [1]. Examples include single-user matched filter receivers, decorrelating detectors, minimum mean-square error (MMSE) linear multiuser detectors, decision-feedback multiuser detectors, successive cancellers, and multistage detectors. Optimum maximum-likelihood (ML) detection, while superior in performance, is not a practical option because of its high complexity.

In this paper, we introduce a class of remarkably efficient multipass multiuser detectors that is a particularly attractive alternative to conventional detectors. These new detectors, which can be related to the iterated-decision equalizers developed in [2], are structurally similar to multistage detectors [3] in that they both generate tentative decisions for all users at each iteration and subsequently use these to cancel MAI at the next iteration. However, unlike the heuristically motivated multistage detectors, these new iterated-decision multiuser detectors take into account the reliability of tentative decisions and are optimized to maximize the signal-to-interference+noise (SINR) ratio at each iteration. We show that these new detectors can achieve asymptotically optimum performance while retaining surprisingly low complexity.

2. CHANNEL MODEL

For the purposes of illustration (and to simplify exposition), we consider a P-user discrete-time synchronous channel model, where the ith user modulates an M-ary PSK symbol x_i onto a randomly generated signature sequence $\mathbf{h}_i = [h_i[1], h_i[2], \ldots, h_i[Q]]^T$ of length Q assigned to that user, where the taps of the sequence are mutually independent, zero-mean, complex-valued, circularly symmetric Gaussian random variables with variance $1/Q$. The received signal is

$$\mathbf{r} = \mathbf{H}\mathbf{A}\mathbf{x} + \mathbf{w}, \tag{1}$$

where $\mathbf{H} = [\mathbf{h}_1|\cdots|\mathbf{h}_P]$ is the $Q \times P$ matrix of signatures, $\mathbf{A} = \mathrm{diag}\{A_1, \ldots, A_P\}$ is the $P \times P$ diagonal matrix of received amplitudes, $\mathbf{x} = [x_1, x_2, \ldots, x_P]^T$ is the $P \times 1$ vector of data symbols, and $\mathbf{w}$ is a Q-dimensional Gaussian vector with independent zero-mean, complex-valued, circularly symmetric components of variance $\mathcal{N}_0$.

3. THE ITERATED-DECISION MULTIUSER DETECTOR

The iterated-decision multiuser detector we now develop processes the received data in an iterative fashion. Specifically, during each iteration or "pass," the received data is premultiplied by a matrix, and tentative decisions made in the previous iteration are then used to construct and subtract out an estimate of the MAI. The resulting MAI-reduced data is then passed on to a slicer, which makes a new set of tentative decisions. With each successive iteration, increasingly refined hard decisions are generated using this strategy.

The structure of the iterated-decision multiuser detector is depicted in Fig. 1, with the parameters of all systems and signals corresponding to the lth pass denoted using the superscript l. On the lth pass of the equalizer where $l = 1, 2, 3, \ldots$, the received vector $\mathbf{r}$ is first premultiplied by a $P \times Q$ matrix $\mathbf{B}^{l\dagger} = [\mathbf{b}_1^l|\cdots|\mathbf{b}_P^l]^\dagger$, producing the $P \times 1$ vector $\tilde{\mathbf{r}}^l = \mathbf{B}^{l\dagger}\mathbf{r}$. Next, an appropriately constructed estimate $\hat{\mathbf{z}}^l$ of the MAI is subtracted from $\tilde{\mathbf{r}}^l$ to produce $\tilde{\mathbf{x}}^l$, i.e., $\tilde{\mathbf{x}}^l = \tilde{\mathbf{r}}^l - \hat{\mathbf{z}}^l$ where $\hat{\mathbf{z}}^l = \mathbf{D}^{l\dagger}\hat{\mathbf{x}}^{l-1}$ with $\mathbf{D}^l = [\mathbf{d}_1^l|\cdots|\mathbf{d}_P^l]$, a $P \times P$ matrix. Since $\hat{\mathbf{z}}^l$ is intended to be some kind of MAI estimate, we restrict attention to the case in which the diagonal el-

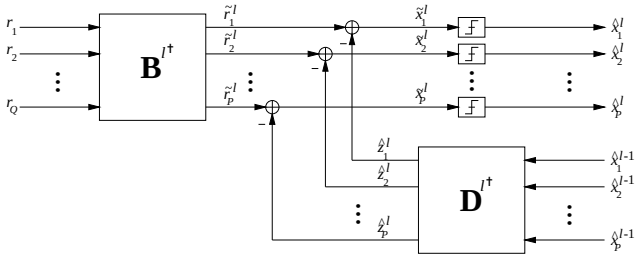

Fig. 1. Iterated-decision multiuser detector structure.

This work has been supported in part by Qualcomm, Inc., the Army Research Laboratory under Cooperative Agreement DAAL01-96-2-0002, and Sanders, a Lockheed-Martin Company.

ements of $\mathbf{D}^l$ are zero. Finally, a bank of slicers then generates the $P \times 1$ vector of hard decisions $\hat{\mathbf{x}}^l$ from $\tilde{\mathbf{x}}^l$ using a minimum-distance rule.

When $\mathbf{x}$ and $\hat{\mathbf{x}}^{l-1}$ are vectors of zero-mean uncorrelated symbols, each with energy $\mathcal{E}_s$, such that their normalized correlation matrix is of the form

$$\frac{E[\mathbf{x} \cdot \hat{\mathbf{x}}^{l-1^\dagger}]}{\mathcal{E}_s} \approx \boldsymbol{\rho}^{l-1} \triangleq \mathrm{diag}\{\rho_1^{l-1}, \rho_2^{l-1}, \ldots, \rho_P^{l-1}\}, \quad (2)$$

then the slicer input for the ith user at the lth iteration can be expressed as

$$\tilde{x}_i^l = \mathbf{b}_i^{l\dagger} \mathbf{h}_i A_i x_i + v_i^l \quad (3)$$

where v_i^l is complex-valued, marginally Gaussian, zero-mean, and uncorrelated with x_i, whose variance is a function of $\mathbf{b}_i^l$ and $\mathbf{d}_i^l$.

The second order model (3) turns out to be a useful one for analyzing and optimizing the performance of the iterated-decision multiuser detector. In particular, during the lth pass, the SINR at each slicer input, defined as $\gamma_i^l(\mathbf{b}_i^l, \mathbf{d}_i^l) = \mathcal{E}_s |\mathbf{b}_i^{l\dagger} \mathbf{h}_i A_i|^2 / \mathrm{var}\ v_i^l$ for $i = 1, 2, \ldots, P$, achieves a maximum value of [4]

$$\gamma_i^l = \left(\frac{1}{([\mathbf{I} + \boldsymbol{\alpha}^l]^{-1})_{ii}} - 1 \right) \cdot \frac{1}{1 - |\rho_i^{l-1}|^2} \quad (4)$$

when[1]

$$\mathbf{B}^l \propto [\mathcal{N}_0 \mathbf{I} + \mathcal{E}_s \mathbf{H}\mathbf{A}(\mathbf{I} - \boldsymbol{\rho}^{l-1}\boldsymbol{\rho}^{l-1^\dagger})\mathbf{A}^\dagger \mathbf{H}^\dagger]^{-1} \mathbf{H}\mathbf{A} \quad (5)$$

$$\mathbf{D}^l = \boldsymbol{\rho}^{l-1^\dagger} \left[\mathbf{B}^{l\dagger} \mathbf{H}\mathbf{A} - \mathrm{diag}\left\{ (\mathbf{B}^{l\dagger}\mathbf{H}\mathbf{A})_{11}, \ldots, (\mathbf{B}^{l\dagger}\mathbf{H}\mathbf{A})_{PP} \right\} \right]^\dagger, \quad (6)$$

where $\boldsymbol{\alpha}^l = \mathcal{E}_s(\mathbf{I} - \boldsymbol{\rho}^{l-1}\boldsymbol{\rho}^{l-1^\dagger})\mathbf{A}^\dagger \mathbf{H}^\dagger \mathbf{H}\mathbf{A}/\mathcal{N}_0$ and $\mathbf{I}$ is the identity matrix.

This result for $\mathbf{d}_i^l$ is intuitively satisfying. If $\hat{x}_i^{l-1} = x_i$ so that $\rho_i^{l-1} = 1$, then the inner product $\mathbf{d}_i^{l\dagger} \hat{\mathbf{x}}^{l-1}$ exactly reproduces the MAI component of $\tilde{r}_i^l$. More generally, ρ_i^{l-1} describes our confidence in the quality of the estimate $\hat{x}_i^{l-1}$. If $\hat{x}_i^{l-1}$ is a poor estimate of x_i, then ρ_i^{l-1} will in turn be low, and a smaller weighting is applied to the MAI estimate that is to be subtracted from $\tilde{r}_i^l$. On the other hand, if $\hat{x}_i^{l-1}$ is an excellent estimate of x_i, then $\rho_i^{l-1} \approx 1$, and nearly all of the MAI is subtracted from $\tilde{r}_i^l$. Note that the diagonal of $\mathbf{D}^l$ is indeed zero, as stipulated previously.

Some comments can be made about the special case of $l = 1$. During the first pass, MAI subtraction is not performed because $\boldsymbol{\rho}^0 = \mathbf{0}$, so the vector $\hat{\mathbf{x}}^0$ does not need to be defined. Moreover, the matrix $\mathbf{B}^1$ reduces to an expression for the linear MMSE multiuser detector. Thus, the performance of the iterated-decision multiuser detector, after just one iteration, is identical to that of the linear MMSE multiuser detector. In Section 4, we show that the iterated-decision multiuser detector, after multiple iterations, performs significantly better than the linear MMSE detector.

Next, the properties of v_i^l suggest that the probability of symbol error for the ith user at the lth iteration can be approximated by the high signal-to-noise ratio (SNR) formula for the M-ary PSK symbol error rate of a symbol-by-symbol threshold detector for additive white Gaussian noise (AWGN) channels, given by [5]

$$\Pr(\epsilon^l) = 2\mathcal{Q}\left(\sin\left(\frac{\pi}{M}\right) \sqrt{2\gamma^l} \right), \quad (7)$$

[1]Using a matrix identity, we may alternatively write

$$\mathbf{B}^l \propto \mathbf{H}\mathbf{A}[\mathcal{N}_0 \mathbf{I} + \mathcal{E}_s(\mathbf{I} - \boldsymbol{\rho}^{l-1}\boldsymbol{\rho}^{l-1^\dagger})\mathbf{A}^\dagger \mathbf{H}^\dagger \mathbf{H}\mathbf{A}]^{-1},$$

which may be easier to evaluate depending on P and Q.

where $\mathcal{Q}(v) = \frac{1}{\sqrt{2\pi}} \int_v^\infty e^{-t^2/2} dt$. For the special case of QPSK ($M = 4$), the exact probability of symbol error at the lth iteration is given by [5]

$$\Pr(\epsilon^l) = \mathcal{Q}\left(\sqrt{\gamma^l}\right) \left[2 - \mathcal{Q}\left(\sqrt{\gamma^l}\right) \right]. \quad (8)$$

For the case of accurate power control, i.e., $\mathbf{A} = A\mathbf{I}$ so $\boldsymbol{\rho}^{l-1} = \rho^{l-1}\mathbf{I}$), in the large system limit ($P \to \infty$ with $\beta \triangleq P/Q$ held constant), the SINR in (4) for each user converges in the mean-square sense to [4]

$$\gamma^l = \left(\frac{1}{1 - \frac{\xi^l}{4\beta} \cdot \mathcal{F}(1/\xi^l, \beta)} - 1 \right) \cdot \frac{1}{1 - |\rho^{l-1}|^2} \quad (9)$$

where $\mathcal{F}(y, z) = (\sqrt{y(1+\sqrt{z})^2 + 1} - \sqrt{y(1-\sqrt{z})^2 + 1})^2$ and $1/\xi^l = \mathcal{E}_s(1 - |\rho^{l-1}|^2)|A|^2/\mathcal{N}_0$. The iterative algorithm for computing the set of correlation coefficients ρ^l, and in turn predicting the sequence of symbol error probabilities is as follows.

1. Set $\rho^0 = 0$ and let $l = 1$.
2. Compute the SINR γ^l from ρ^{l-1} via (9). [It is worth pointing out that for systems with few users, we can alternatively (and in some cases more accurately) compute γ^l from ρ^{l-1} via (4).]
3. Compute $\Pr(\epsilon^l)$ from γ^l via (7).
4. Compute ρ^l via the approximation [4]

$$\rho^l \approx 1 - 2\sin^2\left(\frac{\pi}{M}\right) \Pr(\epsilon^l). \quad (10)$$

5. Increment l and go to step 2.

In the special case of QPSK, it can be shown that the algorithm can be streamlined by eliminating Step 3 and replacing the approximation (10) with the exact formula

$$\rho^l = 1 - 2\mathcal{Q}\left(\sqrt{\gamma^l}\right). \quad (11)$$

4. PERFORMANCE

In this section, we focus exclusively on the case of accurate power control.

From Steps 2 and 3 of the algorithm, we see that $\Pr(\epsilon^l)$ can be expressed as $\Pr(\epsilon^l) = \mathcal{G}(\zeta, \beta, \rho^{l-1})$, where $\mathcal{G}(\cdot, \cdot, \cdot)$ is a monotonically decreasing function in both SNR $1/\zeta$ and correlation ρ^{l-1}, but a monotonically increasing function in β. The monotonicity of $\mathcal{G}(\cdot, \cdot, \cdot)$ is illustrated in Fig. 2 where the solid curves plot $\mathcal{G}(\zeta, \beta, \rho)$ as a function of $1/(1-\rho)$ for various values of β. Meanwhile, from Step 4 of the algorithm, we see that we can also express $\Pr(\epsilon^l)$ as $\Pr(\epsilon^l) = \mathcal{H}(\rho^l)$, where $\mathcal{H}(\cdot)$ is a monotonically decreasing function of ρ^l. The dashed line in Fig. 2 plots $\mathcal{H}(\rho)$ as a function of $1/(1-\rho)$.

For a given $1/\zeta$ and β, the sequence of error probabilities $\Pr(\epsilon^l)$ and correlation coefficients ρ^l can be obtained by starting at the left end of the solid curve (corresponding to $\rho^0 = 0$) and then successively moving horizontally to the right from the solid curve to the dashed line, and then moving downward from the dashed line to the solid curve. Each "step" of the resulting descending staircase corresponds to one pass of the multiuser detector. In Fig. 2, the sequence of operating points is indicated on the solid curves with the $\circ$ symbols.

That the sequence of error probabilities $\Pr(\epsilon^1), \Pr(\epsilon^2), \ldots$ obtained by the recursive algorithm is monotonically decreasing

suggests that additional iterations always improve performance. The error rate performance for a given SNR of $1/\zeta$ and a given β eventually converges to a steady-state value of $\Pr(\epsilon^\infty)$, which is the unique solution to the equation

$$\Pr(\epsilon^\infty) = \mathcal{G}(\zeta, \beta, \mathcal{H}^{-1}(\Pr(\epsilon^\infty))), \tag{12}$$

corresponding to the intersection of the dashed line and the appropriate solid curve in Fig. 2.

If β is relatively small, Fig. 2 suggests that steady-state performance is approximately achieved with comparatively few iterations, after which additional iterations provide only negligibly small gains in performance. This observation can also be readily made from Fig. 4, where bit-error rate is plotted as a function of SNR per bit for $1, 2, 3, 5$, and an infinite number of iterations, with $\beta = 0.77$. It is significant that, for small β, few passes are required to converge to typical target bit-error rates, since the amount of computation is directly proportional to the number of passes required; we emphasize that the complexity of a single pass of the iterated-decision multiuser detector is comparable to that of the decorrelating detector or the linear MMSE multiuser detector.

As β increases, Fig. 2 shows that the gap between the solid curve and the dashed curve decreases. Thus the "steps" of the descending staircase get smaller, and there is a significant increase in the number of iterations required to approximately achieve steady-state performance. Moreover, the probability of error at steady-state becomes slightly larger.

When β is greater than some SNR-dependent threshold, not only can (12) have multiple solutions, but one of the solutions occurs at a high probability of error, as illustrated by the curve in Fig. 2 corresponding to $\beta = 4$. The dependence of the threshold on SNR is shown in Fig. 5. As the SNR increases, the β threshold increases and the curve becomes much sharper at the threshold.

In Fig. 6, we compare the theoretical and simulated bit-error rates of the iterated-decision multiuser detector with the bit-error rates of various other multiuser detectors as a function of SNR, with $\beta = 1$ and power control. The iterated-decision multiuser detector significantly outperforms the other detectors at moderate to high SNR, and asymptotically approaches the matched filter bound for the single-user channel. Thus, perfect MAI cancellation is approached at high SNR.

Next, in Fig. 7, we compare the effect of β on the bit-error rates of the various multiuser detectors when decoding $P = 128$ simultaneous users at an SNR per bit of 7 dB with power control. The iterated-decision multiuser detector has clearly superior performance when $\beta \lesssim 2$.

5. CODED AND ADAPTIVE IMPLEMENTATIONS

For coded systems, an iterated-decision multiuser decoder is readily obtained (Fig. 3), and takes a form analogous to the iterated-decision equalizer-decoder structure described in [2]. The data streams $x_i[n]$, $i = 1, 2, \ldots, P$ of the P users are encoded using separate encoders, and the corresponding streams of coded symbols can be thought of as rows of a $P \times N$ matrix $\bar{\mathbf{X}} = [\bar{\mathbf{x}}[1]|\cdots|\bar{\mathbf{x}}[N]]$. The receiver obtains a set of vectors, one for each symbol period having the form

$$\mathbf{r}[n] = \mathbf{H}\mathbf{A}[n]\bar{\mathbf{x}}[n] + \mathbf{w}[n] \qquad \text{for } n = 1, 2, \ldots, N. \tag{13}$$

At the receiver, the $Q \times N$ matrix of the received vectors, $\mathbf{R} = [\mathbf{r}[1]|\cdots|\mathbf{r}[N]]$, is processed in an iterative fashion. Each $Q \times 1$ column of $\mathbf{R}$, which represents a particular symbol period, can be processed independently to produce a $P \times 1$ column of the matrix $\tilde{\mathbf{X}}^l = [\tilde{\mathbf{x}}^l[1]|\cdots|\tilde{\mathbf{x}}^l[N]]$. Each $1 \times N$ row of the matrix $\tilde{\mathbf{X}}^l$, corresponding to the data for a particular user, is then input to a soft-decision ML decoder, which produces a row in the $P \times N$ matrix $\hat{\mathbf{X}}^l = [\hat{\mathbf{x}}^l[1]|\cdots|\hat{\mathbf{x}}^l[N]]$, the tentative decisions for the P users. These tentative decisions must be re-encoded before being processed by the matrix $\mathbf{D}^{l^\dagger}[n]$.

Adaptive implementations can likewise be developed in a manner analogous to those described in [2] and [1, 6].

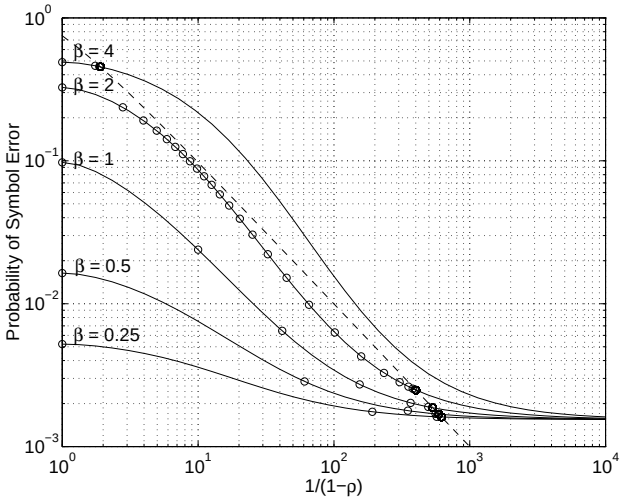

Fig. 2. Theoretical iterated-decision multiuser detector performance, with power control. The solid curves plot QPSK symbol error rate as a function of the correlation coefficient ρ for various values of $\beta = P/Q$, with an SNR per bit of 7 dB. Along each curve, $\circ$'s identify the theoretically predicted decreasing error rates achieved with $l = 1, 2, \ldots$ decoding passes, and the intersections with the dashed line are the steady-state values ($l \to \infty$).

6. REFERENCES

[1] S. Verdú, *Multiuser Detection*. Cambridge, U.K.: Cambridge Univ. Press, 1998.

[2] A. M. Chan and G. W. Wornell, "A class of block-iterative equalizers for intersymbol interference channels," in *Int. Conf. Commun.,* (New Orleans, LA), June 2000.

[3] M. K. Varanasi and B. Aazhang, "Near-optimum detection in synchronous code-division multiple-access systems," *IEEE Trans. Commun.*, vol. 39, pp. 725–736, May 1991.

[4] A. M. Chan and G. W. Wornell, "A new class of efficient block-iterative interference cancellation techniques for digital communication receivers," to appear in *J. VLSI Signal Process.*, special issue on *Signal Processing for Wireless Communication: Algorithms, Performance, and Architectures*. (invited paper)

[5] J. G. Proakis, *Digital Communications*, 3rd ed. New York: McGraw-Hill, 1995.

[6] M. L. Honig and H. V. Poor, "Adaptive interference suppression" in *Wireless Communications: Signal Processing Perspectives* (H. V. Poor and G. W. Wornell, eds.). Upper Saddle River, NJ: Prentice-Hall, 1998.

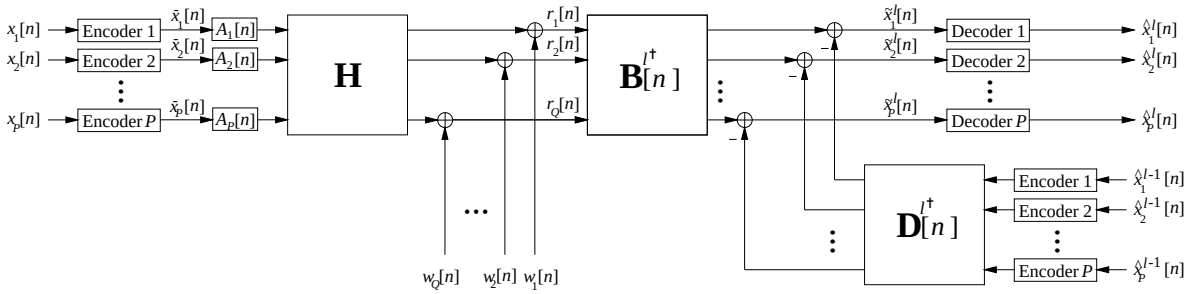

Fig. 3. Structure of a communication system that combines iterated-decision multiuser detection with channel coding.

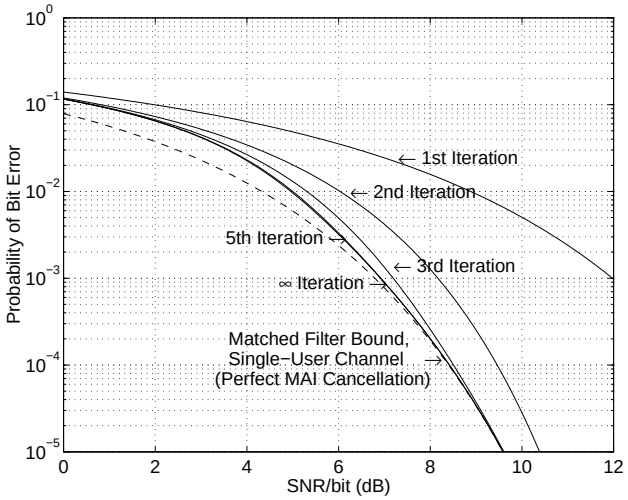

Fig. 4. Theoretical iterated-decision multiuser detector performance with power control, as a function of SNR per bit. The successively lower solid curves depict the QPSK bit-error rate with $\beta = P/Q = 0.77$ as a function of SNR per bit for 1, 2, 3, 5, and ∞ decoding iterations.

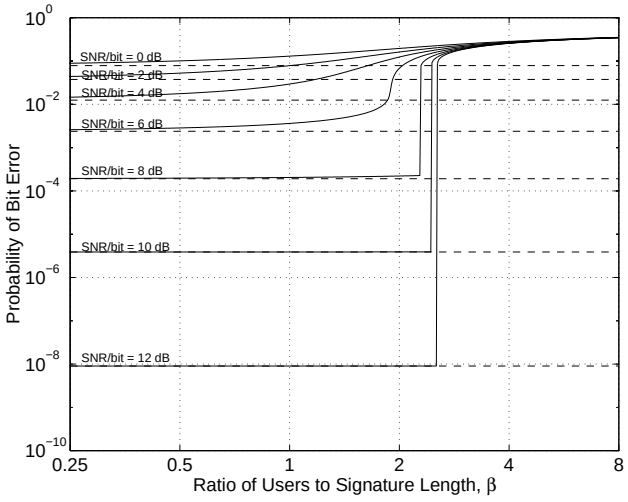

Fig. 5. Theoretical iterated-decision multiuser detector performance with power control, as a function of $\beta = P/Q$. The solid curves depict the QPSK bit-error rate as a function of β for various values of SNR per bit, while the corresponding dashed curves depict the matched filter bound for the single-user channel.

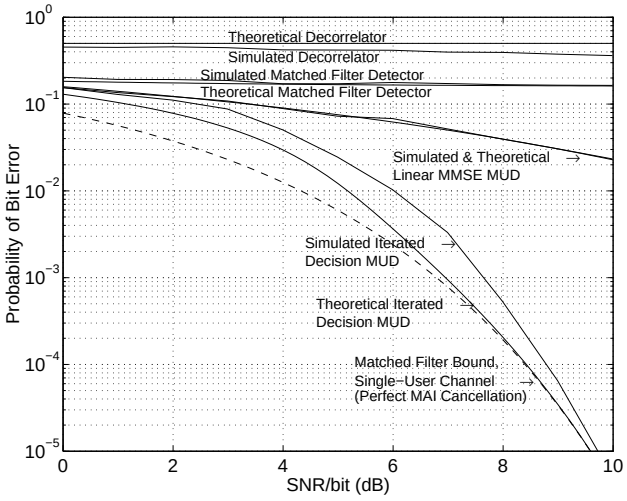

Fig. 6. Theoretical ($Q \to \infty$) and experimentally observed ($Q = 128$) performance for various multiuser detectors, with power control. The solid curves depict QPSK bit-error rates with $\beta = P/Q = 1$ as a function of SNR per bit.

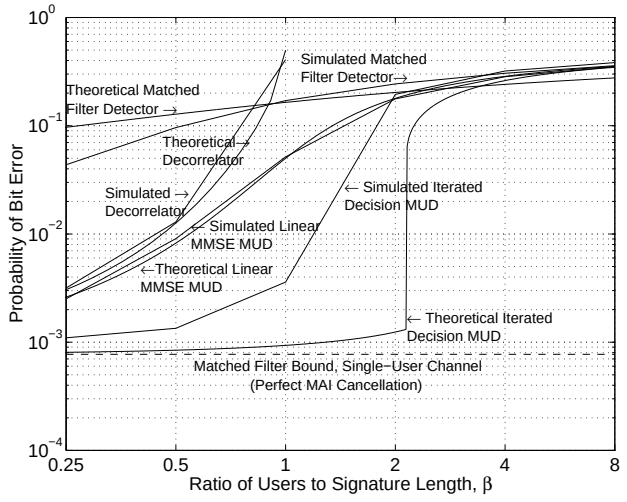

Fig. 7. Theoretical ($Q \to \infty$) and experimentally observed ($Q = 128$) performance for various multiuser detectors, with power control. The solid curves depict QPSK bit-error rates at an SNR per bit of 7 dB as a function of $\beta = P/Q$.